ACS APPLIED MATERIALS & INTERFACES

LETTER

www.acsami.org

Interface Toughness of Carbon Nanotube Reinforced Epoxy Composites

Yogeeswaran Ganesan,[†] Cheng Peng,[†] Yang Lu,[†] Phillip E. Loya,[†] Padraig Moloney,[†] Enrique Barrera,[†] Boris I. Yakobson,[†,‡] James M. Tour,[†,‡] Roberto Ballarini,[*,§] and Jun Lou[*,†]

[†]Department of Mechanical Engineering and Materials Science and [‡]Department of Chemistry, Rice University, 6100 Main Street, Houston, Texas 77005, United States

[§]Department of Civil Engineering, University of Minnesota, Minneapolis, Minnesota 55455, United States

Supporting Information

ABSTRACT: Traditional single-fiber pull-out type experiments were conducted on individual multiwalled carbon nanotubes (MWNT) embedded in an epoxy matrix using a novel technique. Remarkably, the results are qualitatively consistent with the predictions of continuum fracture mechanics models. Unstable interface crack propagation occurred at short MWNT embedments, which essentially exhibited a linear load−displacement response prior to peak load. Deep embedments, however, enabled stable crack extension and produced a nonlinear load−displacement response prior to peak load. The maximum pull-out forces corresponding to a wide range of embedments were used to compute the nominal interfacial shear strength and the interfacial fracture energy of the pristine MWNT-epoxy interface.

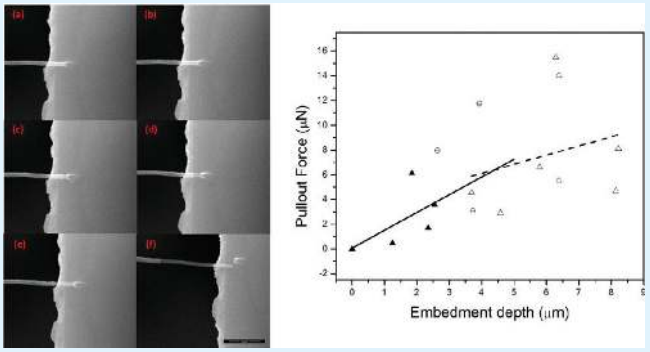

KEYWORDS: multiwall carbon nanotubes, epoxy composite, single-fiber pull-out, interfacial strength

INTRODUCTION

The effectiveness of a fiber in improving the mechanical behavior of a composite depends primarily on the mechanical properties of the fiber and the strength/toughness of the fiber-matrix interface. Carbon nanotubes (CNTs) are low density materials that possess high strength (as high as 30−110 GPa[1,2]) and stiffness (~1 TPa[3]) and thus offer promise as reinforcements for strong, stiff, tough and lightweight composites. However, their atomically smooth surface and their limited ability to form covalent bonds with a surrounding matrix material limits the extent of nanomechanical interlocking and interfacial strength, respectively. Whatever strength is exhibited by the interface in CNT reinforced composites is attributed to nonbond interactions, such as van der Waals forces, electrostatic interactions, and the confinement arising from thermal mismatch.[4] There have been conflicting reports, primarily based on theoretical models or simulations, on the nature of nonbond interactions, and in particular on their effects on adhesion at the interface.[5] CNT dimensions and the forces and displacements required to pull them out of a matrix are so small that sufficient experimental data and a quantitative understanding of CNT/matrix interfaces, required to design a composite that behaves as desired, is lacking.

Single fiber pull-out tests have been used since the early development of composite materials technology to measure the shear strength of ductile interfaces capable of developing a constant shear stress prior to fiber pull-out, and the fracture energy of brittle interfaces that experience crack initiation and propagation prior to fiber pull-out. It is for this reason that attempts have been made to perform similar experiments on CNT/matrix composites. Attempts made so far include the use of atomic force microscope (AFM) probes ex situ[6] or in situ within a scanning electron microscope (SEM) chamber.[7] There are several major issues associated with AFM probe-based single CNT pull-out tests, including misalignment that can be exacerbated by natural deviation from the vertical direction during loading of the cantilever-tip assembly. In addition, the extraction of a force signal in AFM probe assisted in situ experiments is based upon estimates of cantilever stiffness and involves the determination of cantilever deflection from low resolution SEM images, both of which can lead to undesirable errors. Lastly, embedment depth cannot be easily controlled and/or measured using such techniques.

We have developed a novel and robust micromechanical testing platform that, working in conjunction with a quantitative nanoindenter, enabled us to perform in situ pull-out tests within a scanning electron microscope (SEM) chamber on single MWNTs

Received: November 13, 2010
Accepted: December 28, 2010
Published: January 7, 2011

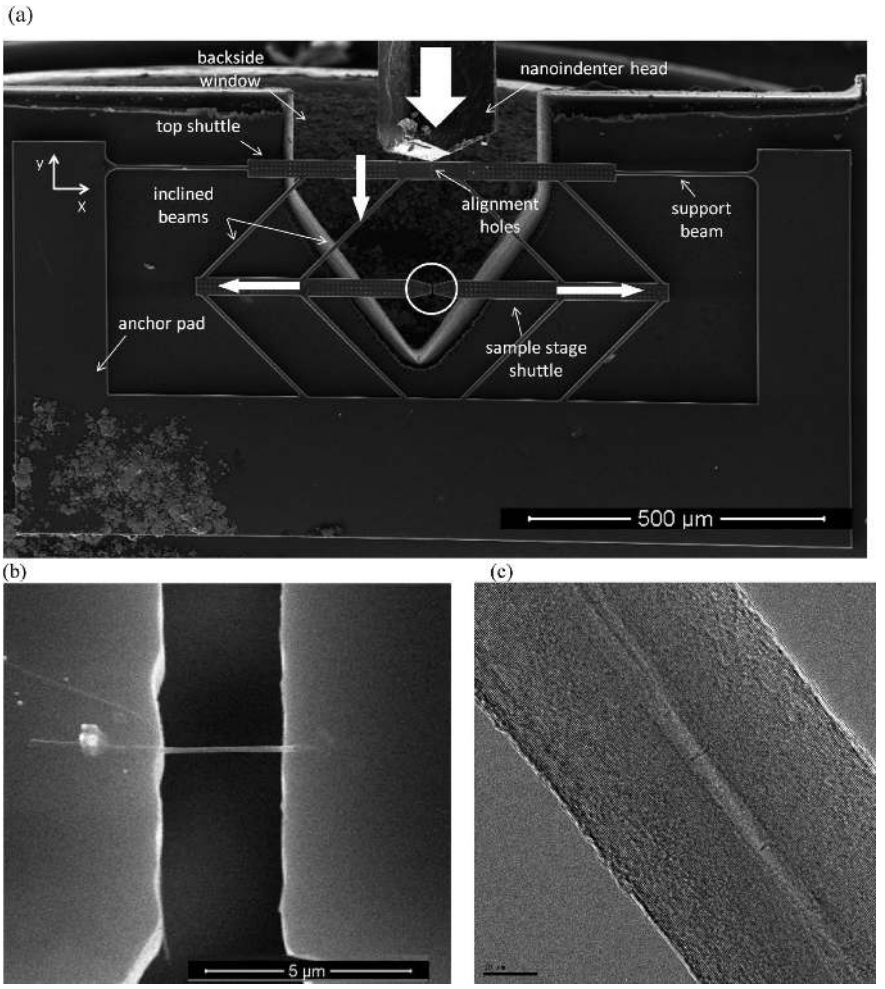

Figure 1. Figure shows testing techniques employed and images of specimens (a) SEM micrograph of microfabricated device used to perform the pull-out experiments. Block arrows show the direction of movement of the indenter and the shuttles. (b) Close up SEM image of the circled region in panel a showing a MWNT pull-out specimen before the start of the experiment. (c) TEM image of MWNT. (Scale bar reads 100 nm.)

embedded within an epoxy matrix.[8,9] The nanoindenter-assisted testing platform is essentially a miniaturized version of a traditional pull-out experiment, and thus allows for the application and measurement of purely axial forces and displacements, albeit with nano-Newton and nanometer resolution. The force and displacements can be measured independently (the force application and displacement measurement resolution of the Agilent in SEM G200 nanoindenter are 69.4 nN and 0.8675 nm, respectively, as estimated from noise floor measurements) thus facilitating real time observation of the single fiber pull-out process. The procedure also allows the facile implementation of desired fiber embedment depths and composite processing conditions, such as room temperature cure followed by high-temperature post cure.

RESULTS AND DISCUSSION

The microdevice shown in Figure 1a is a spring-like "push-pull" mechanism consisting of three movable shuttles attached to each other via inclined freestanding beams. Loading of the pull-out specimen held on the sample stage shuttle is achieved by using a nanoindenter to apply a downward displacement to the top shuttle, which four sets of inclined symmetrical beams transform into a two-dimensional translation of the sample stage shuttles. Proper alignment of the nanoindenter head ensures that the stress applied to the specimen, mounted across the sample stage shuttles and shown in Figure 1b, is purely axial. The pull-out specimens used in this study are comprised of individual MWNTs (Mitsui Corp., Japan, lot no. 05072001K28) (see Figure 1c) embedded in Epon 828 epoxy films covering certain sections of the sample stage shuttles of the micromechanical devices. Epon 828 was chosen as the matrix material because it is routinely used as a standard resin for formulation, fabrication and fusion technology. The specimen preparation procedure is described in detail in the Supporting Information section. Application of μN-level loads resulted in the pull-out of the MWNT specimens from the epoxy matrix, as observed in the SEM snapshots extracted from the video recording of an illustrative test shown in Figure 2.

Figure 3a and b provides representative load−displacement plots that were extracted from the corresponding nanoindenter load vs displacement curves, using a simple response subtraction procedure.[10] Response subtraction essentially involves the ascertainment of forces needed to displace the pull-out specimens by subtracting the forces needed to deform the device alone from the forces needed to deform the device in the presence of the specimen. It was observed that the response before the maximum load was reached was linear for short embedment depths and

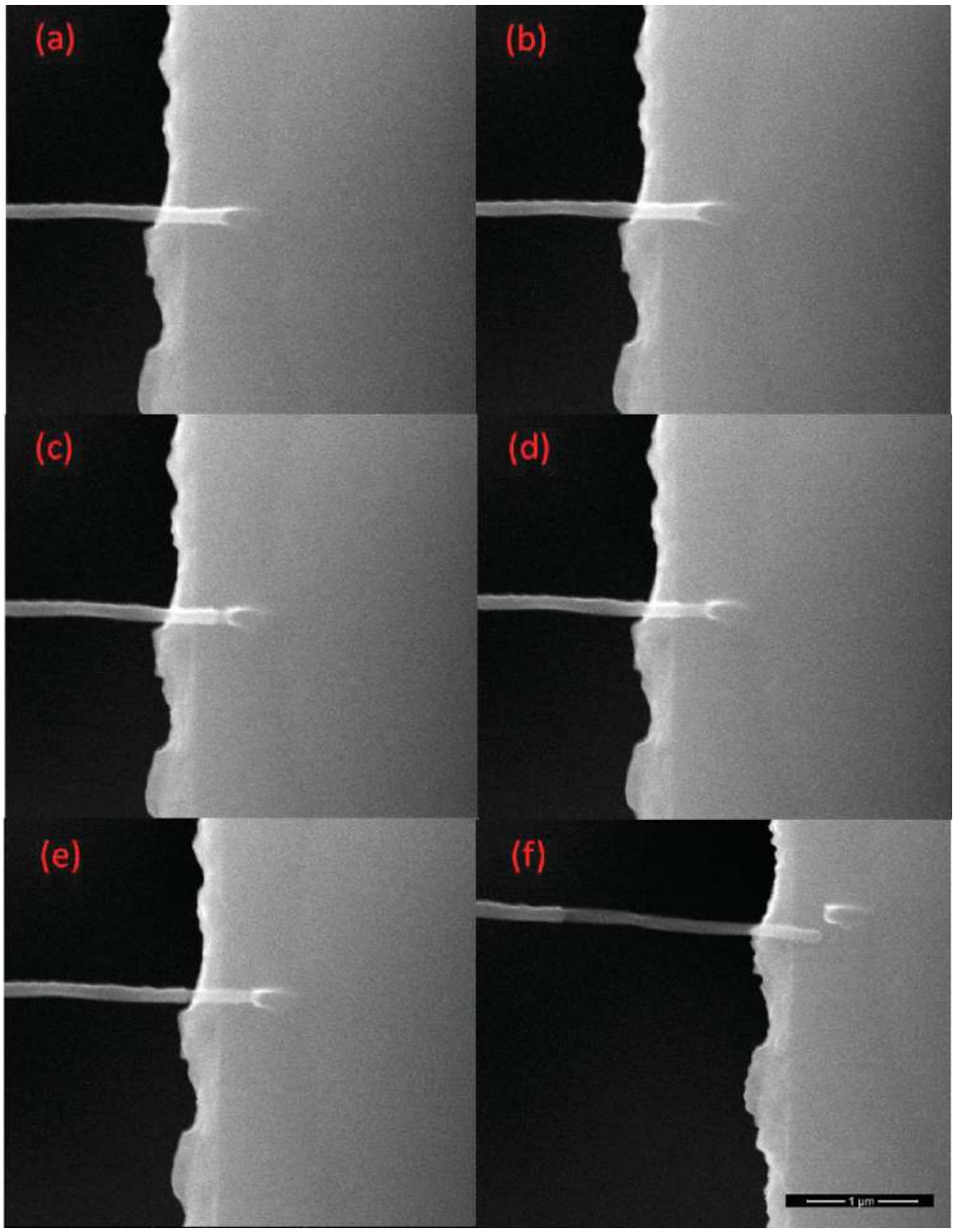

Figure 2. SEM snapshots showing a single MWNT as it pulls out of an epoxy matrix at (a) $t = 0$, (b) $t = 10$, (c) $t = 19$, (d) $t = 30$, (e) $t = 70$, and (f) $t = 300$ s, respectively. The experiment was conducted at an indenter displacement rate of 10 nm/s.

nonlinear for large embedments. Figure 4 shows the maximum pull-out force measured on 15 samples representing a wide range of embedments. As expected for single fiber pull-out experiments,[11] the data exhibits considerable scatter. The pull-out force values were used to calculate the nominal shear strength of the interface (see Table 1), defined as

$$\tau = \frac{P_c}{2\pi r l} \quad (1)$$

where P_c is the experimentally measured maximum pull-out force, r is the MWNT radius, and l is the embedment depth. It is observed that τ exhibits significant scatter, and that its average value of 6.24 ± 3.6 MPa is 1 order of magnitude lower than the 62 MPa tensile strength of the polymer matrix and orders of magnitudes lower than the strength of the MWNTs (see Supporting Information). It is worth noting that single-fiber pull-out experiments are inherently prone to data scattering. The origin of the data scattering had been assumed to be experimental error associated with pull-out testing, though fracture mechanics analysis suggests that the data scattering is also inherent in the specimens themselves.[11] The scatter apparently becomes particularly pronounced when nanoscale fibers are used as reinforcements. Experiments similar to the ones described in the manuscript, conducted in the past (MWNT-polyethene-butene system), revealed a similar scatter in the data.[6] It is postulated that the scatter arises partially due to the fact that minor variations that occur during specimen preparation have a substantial effect on the values of maximum pullout load obtained.

The lack of dependence of pull-out capacity on embedment depth implies that the pull-out process is not ductile (a constant

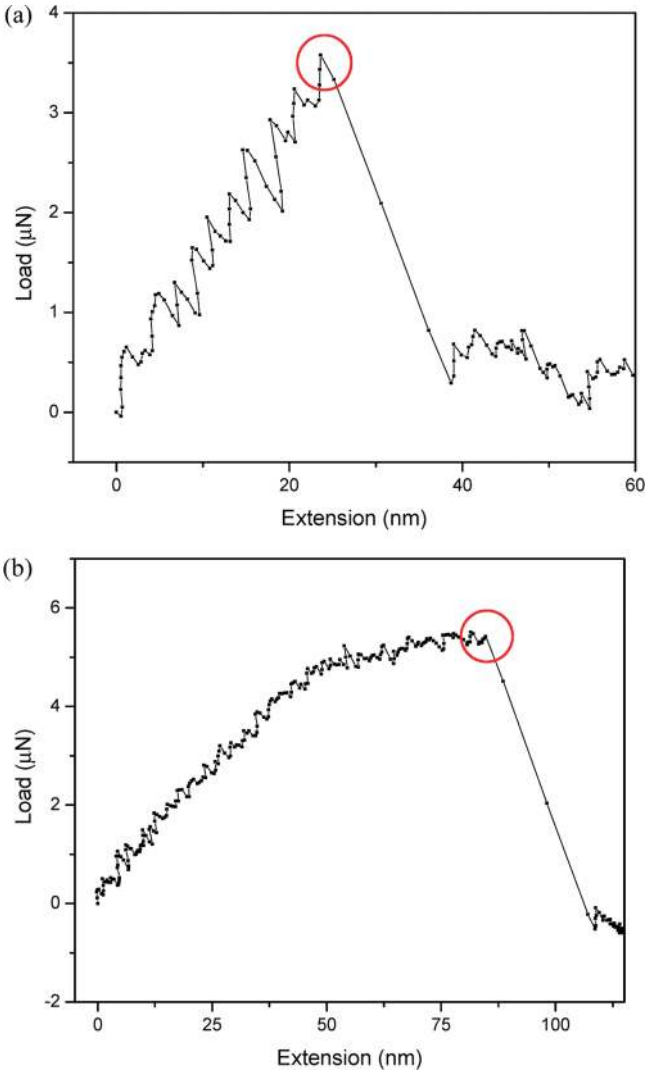

Figure 3. Representative load−extension curves for (a) a specimen with a small embedment (2.55 um) and (b) a specimen with large embedment (6.38 um). Circles indicate the maximum pull-out load values.

shear stress equal to τ is not developed along the interface), but instead is associated with brittle cracking. The crack propagation scenario is supported also by the shapes of the load−displacement plots. Consistent with predictions of continuum fracture mechanics models, fibers with short embedments pull-out as a result of catastrophic (unstable) propagation of an initiated interface crack and exhibit a linear prepeak response (see Figure 3a and Table 1). Deep embedments experienced subcritical crack extension along the interface prior to peak load, resulting in a continuous reduction in stiffness that is reflected by a nonlinear load−displacement response (see Figure 3b and Table 1).

The experimental results suggest that the pull-out experiments can provide the interfacial fracture energy using the approximate fracture mechanics model developed by Jiang and Penn.[12] Neglecting the effects of matrix compression and assigning a zero value of friction coefficient to the analytical formulas in ref 12 leads to the following formula relating the maximum pull-out force, P_c, the Young's modulus of the fiber (matrix), E_f (E_m), the Poisson's ratio of the matrix, υ_m, the radial distance from the fiber axis at which the shear stress in the matrix reduces to zero, R,

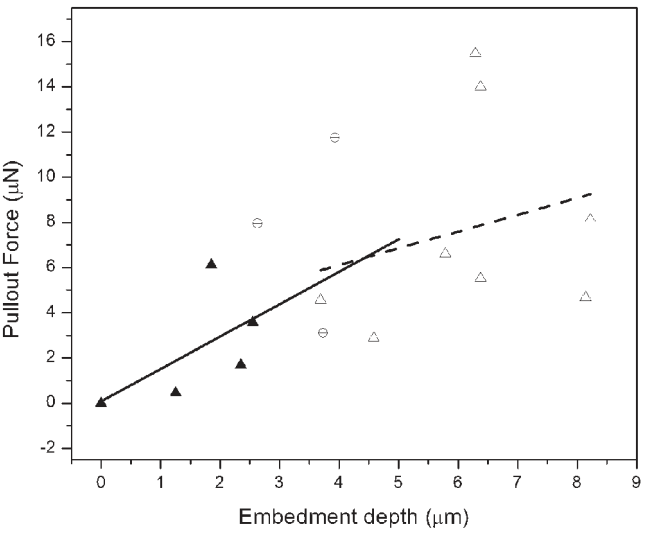

Figure 4. Maximum pull-out force versus nanotube embedded depth. The symbol (▲) indicates points that correspond to embedments that exhibited a linear pull-out load−displacement response. The symbol (Δ) indicates points corresponding to deep embedments that exhibited a nonlinear pull-out load−displacement response. The symbol (⊖) indicates points corresponding to embedments that did not exhibit a clearly linear or nonlinear pull-out load−displacement response. Also shown are the linear fits that were applied for the points indicated by (▲) (solid line) and the points indicated by (Δ) (dashed line); their point of convergence was used to determine l_{th}, (4.42 μm), and its corresponding maximum pull-out force value P_c, namely, (6.42 μN).

the embedment depth, l, the initial crack length at the interface, a, and the MWNT radius, r

$$P_c = \frac{2\pi r\sqrt{rE_f G_c}}{\sqrt{1+\csc h^2\left(n\frac{l-a}{r}\right)}} \quad (2)$$

where n is a utility constant defined as

$$n = \sqrt{\frac{E_m}{E_f(1+\upsilon_m)\ln\frac{R}{r}}}$$

Maximum pull-out force values corresponding to nonlinear load−displacement responses, which were, in turn, associated with deep embedments, can be assumed to be equal to the load required to debond the MWNT from the epoxy plus an amount of energy dissipated by frictional effects between the MWNT and the epoxy over the debonded length. In other words, only the set of measured values of maximum pull-out force corresponding to pull-outs characterized by a linear load−displacement response can be used to compute the value of interfacial fracture energy G_c using eq 2. However, short embedments are known to be susceptible to errors introduced by the presence of initial cracks (formed during specimen preparation or handling, initial cracks that are a large fraction of the embedment depth can reduce the value of P_c substantially). Equation 2 can thus be used to accurately estimate the value of G_c only when the embedment depth is equal to a threshold value, l_{th}, for which the maximum pull-out force value is insensitive to initial crack size and friction, and begins to approach a steady-state value independent of embedment depth. In other words, to determine G_c, one would need to

Table 1. Interfacial Properties Ascertained from Single MWNT Pull-out Experiments

embedment depth (μm)	MWNT outer diameter (nm)	maximum pull-out force (μN)	interfacial shear strength, τ (MPa)	nature of load−displacement response
1.25	64.0	0.46	1.84	linear
1.85	94.4	6.12	11.17	linear
2.35	95.7	1.7	2.41	linear
2.55	93.7	3.58	4.77	linear
2.63	77.3	7.95	12.45	not clear
3.69	70.3	4.55	5.56	nonlinear
3.73	71.8	3.10	3.69	not clear
3.93	95.5	11.75	9.98	not clear
4.58	70.0	2.88	2.86	nonlinear
5.79	53.5	6.61	6.8	nonlinear
6.29	83.5	15.48	9.39	nonlinear
6.38	64.1	14.01	10.91	nonlinear
6.38	61.3	5.51	4.49	nonlinear
8.14	69.3	4.68	2.64	nonlinear
8.22	67.5	8.12	4.66	nonlinear

ascertain the point of transition between the catastrophic interfacial failure mode and the subcritical interfacial crack extension mode (Figure 4).

The average Young's modulus value of the MWNT specimens was obtained by performing tensile tests using the aforementioned microfabricated device (see Supporting Information).[13] Assuming the entire cross sectional area of each nanotube was load bearing (a reasonable assumption since most catalytically grown MWNTs possess intershell cross-links that lead to considerable intershell load transfer[1]), E_f was found to be equal to 200 GPa. The modulus of unreinforced Epon 828 (mixed with Epikure 3200 in a 10:1 ratio) resin was measured using tension experiments conducted on dog-bone shaped resin specimens. The average value E_m was found to be 1.099 GPa. The Poisson's ratio of the resin was set equal to 0.33.[14]

The diameters of the MWNTs were measured as 75 ± 20 nm. Assuming a zero value for the initial crack length at the interface, and a stress transfer parameter R/r value ranging from 2 (a value typical for weak interfaces) to 9 (a value that would be typical for a strong interface),[15,16] eq 2 provides an interfacial fracture energy value for the pristine MWNT-Epon 828 interface within the range of 0.05−0.25 J/m^2. Note that the choice of the value of the stress transfer parameter R/r does not significantly affect the value of G_c; the uncertainty in the fracture energy value arises primarily from the variation in the nanotube diameter.

The value of G_c obtained in our pull-out experiments is approximately 2 orders of magnitude lower than that of other engineered composite materials.[17] It is also considerably lower than the values reported for nanotube pull-out from a polyethylene butene matrix (4−70 J m^{-2}).[6] We note that the nominal shear strength measured from our experiments is considerably lower than the values reported for the MWNT-epoxy (Poxipol^{TM} glue) system[7] (22.26 MPa, based on AFM tip assisted single MWNT pull-out experiments), the MWNT-polyurethane system[18] (500 MPa, based on stress induced fragmentation experiments), the carbon nanofiber-Epikote 862 system[19] (170 MPa, using a probe assisted pull-out technique) and the MWNT-polystyrene system[4] (160 MPa, value obtained via molecular mechanics simulations and elasticity calculations). The nature of the MWNTs (synthesis technique, surface morphology etc.) and the differences in experimental techniques used in the experiments can have a significant impact on the reported interfacial properties of the composite system. It is worth noting that in a separate effort, macro-scale tensile tests were conducted on dog-bone shaped MWNT-epoxy composite specimens. 0.5% (by weight) MWNTs (from the same batch as those used in single fiber pullout experiments) were incorporated into the Epon 828 matrix and the mechanical properties of the composites were tested. The reinforcing effect of the MWNTs was found to be minimal. Also, post-fracture analysis of the specimens revealed that MWNTs consistently pulled out of the matrices (MWNT fracture was not observed on the fracture surfaces of the dog-bone specimens, see Supporting Information), thus corroborating the existence of an extremely weak MWNT-Epon 828 interface.

CONCLUSIONS

We thus described how a novel microfabricated device was used within a SEM chamber to perform in situ pull-out experiments on a MWNT/epoxy nanocomposite. Fifteen successful experiments allowed us to measure the interfacial fracture energy, G_c, for the MWNT-Epon 828 interface, which was found to be considerably lower than those reported earlier for similar systems and of those associated with conventional engineering composite systems. The results of this study highlight the extremely weak nature of the adhesive forces that act at the MWNT-Epon 828 interface. Nanomechanical interlocking, covalent bonding and polymer chain wrapping, three factors that generally play a significant role in filler matrix bonding, were assumed to have contributed minimally to adhesion at the MWNT-Epon 828 interface.

ASSOCIATED CONTENT

Supporting Information. Experimental method and additional figures. This information is available free of charge via the Internet at http://pubs.acs.org.

AUTHOR INFORMATION

Corresponding Author

*E-mail: broberto@umn.edu (R.B.); jlou@rice.edu (J.L.). Tel: (216) 368 2963 (R.B.); (713) 348 3573 (J.L.). Fax: (216) 368 5229 (R.B.); (713) 348 5423 (J.L.).

ACKNOWLEDGMENT

The authors would like to acknowledge the support by National Science Foundation grants NSF CMMI 0800896 and 0928297, the Welch Foundation grant C-1716, and the Air Force Research Laboratory grant AFRL FA8650-07-2-5061. This work was also supported in part by the MRSEC Program of the National Science Foundation under Award Number DMR-0819885. The authors thank Mr. Long Chang for help provided with electron beam assisted deposition of platinum, and Mitsui Corp. and Professor M. Endo for the donation of the MWNTs.

REFERENCES

(1) Yu, M. F.; Lourie, O.; Dyer, M. J.; Moloni, K.; Kelly, T. F.; Ruoff, R. S. *Science* **2000**, *287*, 637–640.

(2) Peng, B.; Locascio, M.; Zapol, P.; Li, S.; Mielke, S. L.; Schatz, G. C.; Espinosa, H. D. *Nat. Nanotechnol.* **2008**, *3*, 626–631.

(3) Wong, E. W.; Sheehan, P. E.; Lieber, C. M. *Science* **1997**, *277*, 1971–1975.
(4) Liao, K.; Li, S. *App. Phys. Lett.* **2001**, *79*, 4225–4227.
(5) Ganesan, Y.; Lou, J. *JOM* **2009**, *61* (1), 32–37.
(6) Barber, A. H.; Cohen, S. R.; Kenig, S.; Wagner, H. D. *Compos. Sci. Technol.* **2004**, *64*, 2283–2289.
(7) Barber., A. H.; Cohen, S. R.; Eitan, A.; Schadler, L. S.; Wagner, H. D. *Adv. Mater.* **2006**, *18*, 83–87.
(8) Ganesan, Y.; Lu, Y.; Peng, C.; Lu, H.; Ballarini, R.; Lou, J. *J. Microelectromech. Syst.* **2010**, *19*, 675–682.
(9) Lu, Y.; Ganesan, Y.; Lou, J. *Exp. Mech.* **2010**, *50*, 47–54.
(10) Eppell, S. J.; Smith, B. N.; Kahn, H.; Ballarini, R. *J. R. Soc., Interface* **2006**, *3*, 117–121.
(11) Penn, L. S.; Lee, S. M. *J. Compos. Technol. Res.* **1989**, *11*, 23–30.
(12) Jiang, K. R.; Penn, L. S. *Compos. Sci. Technol.* **1992**, *45*, 89–103.
(13) Ganesan, Y.; Peng, C.; Lu, Y.; Ci, L.; Srivastava, A.; Ajayan, P. M.; Lou, J. *ACS Nano* **2010**, *4*, 7637–7643.
(14) May, C. A. In *Epoxy Resins, Chemistry and Technology*, 2nd ed.; Marcel Dekker: New York, 1988; p 608.
(15) Galiotis, C. *Compos. Sci. Technol.* **1991**, *42*, 125–150.
(16) Detassis, M.; Frydman, E.; Vrieling, D.; Zhou, X. F.; Wagner, H. D.; Nairn, J. A. *Composites, Part A* **1996**, *27*, 769–773.
(17) Zhandarov, S.; Pisanova, E.; Mader, E.; Nairn, J. A. *J. Adhes. Sci. Technol.* **2001**, *15*, 205–222.
(18) Wagner, H. D.; Lourie, O.; Feldman, Y.; Tenne, R. *Appl. Phys. Lett.* **1998**, *72*, 188–190.
(19) Manoharan, M. P.; Sharma, A.; Desai, A. V.; Haque, M. A.; Bakis, C. E.; Wang, K. W. *Nanotechnology* **2009**, *20*, No. 295701(1−5).